TISSUE ENGINEERING: Part A
Volume 19, Numbers 7 and 8, 2013

DOI: 10.1089/ten.tea.2012.0370

CD90 (Thy-1)-Positive Selection Enhances Osteogenic Capacity of Human Adipose-Derived Stromal Cells

Michael T. Chung, BS,[1] Chunjun Liu, MD,[1] Jeong S. Hyun, MD,[1] David D. Lo, MD,[1] Daniel T. Montoro, BS,[1] Masakazu Hasegawa, MD,[1] Shuli Li, PhD,[1] Michael Sorkin, MD,[1] Robert Rennert, BS,[1] Michael Keeney, PhD,[2] Fan Yang, PhD,[2,3] Natalina Quarto, PhD,[1] Michael T. Longaker, MD, MBA,[1,4] and Derrick C. Wan, MD[1]

Background: Stem cell-based bone tissue engineering with adipose-derived stromal cells (ASCs) has shown great promise for revolutionizing treatment of large bone deficits. However, there is still a lack of consensus on cell surface markers identifying osteoprogenitors. Fluorescence-activated cell sorting has identified a subpopulation of $CD105^{low}$ cells with enhanced osteogenic differentiation. The purpose of the present study was to compare the ability of CD90 (Thy-1) to identify osteoprogenitors relative to CD^{105}.
Methods: Unsorted cells, $CD90^+$, $CD90^-$, $CD105^{high}$, and $CD105^{low}$ cells were treated with an osteogenic differentiation medium. For evaluation of *in vitro* osteogenesis, alkaline phosphatase (ALP) staining and alizarin red staining were performed at 7 days and 14 days, respectively. RNA was harvested after 7 and 14 days of differentiation, and osteogenic gene expression was examined by quantitative real-time polymerase chain reaction. For evaluation of *in vivo* osteogenesis, critical-sized (4-mm) calvarial defects in nude mice were treated with the hydroxyapatite-poly(lactic-co-glycolic acid) scaffold seeded with the above-mentioned subpopulations. Healing was followed using micro-CT scans for 8 weeks. Calvaria were harvested at 8 weeks postoperatively, and sections were stained with Movat's Pentachrome.
Results: Transcriptional analysis revealed that the $CD90^+$ subpopulation was enriched for a more osteogenic subtype relative to the $CD105^{low}$ subpopulation. Staining at day 7 for ALP was greatest in the $CD90^+$ cells, followed by the $CD105^{low}$ cells. Staining at day 14 for alizarin red demonstrated the greatest amount of mineralized extracellular matrix in the $CD90^+$ cells, again followed by the $CD105^{low}$ cells. Quantification of *in vivo* healing at 2, 4, 6, and 8weeks postoperatively demonstrated increased bone formation in defects treated with $CD90^+$ ASCs relative to all other groups. On Movat's Pentachrome-stained sections, defects treated with $CD90^+$ cells showed the most robust bony regeneration. Defects treated with $CD90^-$ cells, $CD105^{high}$ cells, and $CD105^{low}$ cells demonstrated some bone formation, but to a lesser degree when compared with the $CD90^+$ group.
Conclusions: While $CD105^{low}$ cells have previously been shown to possess an enhanced osteogenic potential, we found that $CD90^+$ cells are more capable of forming bone both *in vitro* and *in vivo*. These data therefore suggest that CD90 may be a more effective marker than CD105 to isolate a highly osteogenic subpopulation for bone tissue engineering.

Introduction

Skeletal defects resulting from congenital deformities, trauma, degenerative disease, and tumor resection often require large amounts of bone for reconstruction. Bone defects above a critical size, particularly of the adult human skull, do not heal spontaneously, leading to nonunion and the formation of scar tissue. While autogenous bone grafts remain the gold standard for reconstructing large skeletal defects, due to the limited supply of donor sites, alloplastic materials have been used to fill in bone defects. However, the disadvantages of autogenous bone grafts and the increased risk of infection associated with alloplastic materials have fueled the search for an alternative approach to repair large skeletal defects.

[1]Hagey Laboratory for Pediatric Regenerative Medicine, Plastic and Reconstructive Surgery Division, Department of Surgery, Stanford University School of Medicine, Stanford, California.
[2]Stem Cell and Biomaterials Engineering Laboratory, Department of Bioengineering, Stanford, University School of Medicine, Stanford, California.
[3]Department of Orthopaedic Surgery, Stanford University School of Medicine, Stanford, California.
[4]Institute for Stem Cell Biology and Regenerative Medicine, Stanford University, Stanford, California.

Mesenchymal stem cells (MSCs) were first discovered in the bone marrow by Friedenstein *et al.* in 1974.[1,2] Since then, the interest in adult MSCs has progressively grown due to their ability to self-replicate, while maintaining the capacity to differentiate into multiple cell types. In 2001, Zuk *et al.* published the first report of multipotent cells in adipose tissue, naming these processed lipoaspirate cells based on their method of isolation.[3] At around the same time, Gimble and coworkers identified adipose-derived stromal cells (ASCs) that were capable of osteogenic differentiation.[4–6] These cells have many properties that suggest considerable potential utility in cellular therapy for bone repair and regeneration. Importantly, unlike human bone marrow-derived MSCs (BM-MSCs), ASCs can be easily and safely harvested in large quantities with minimal morbidity. The abundance of stem cells in adipose tissue is 100-fold higher than that in the bone marrow and the yield of ASCs after expansion is approximately 400,000 cells per mL of lipoaspirate tissue.[3,7,8]

Like BM-MSCs, ASCs have shown the ability to undergo osteogenic differentiation. However, the freshly isolated stromal vascular fraction (SVF) from adipose tissue contains a mixture of cells, which not only includes ASCs, but also endothelial cells, smooth muscle cells, pericytes, fibroblasts, and other circulating cells.[9] Flow cytometric analysis of ASCs has shown that they share common cell-surface receptors with BM-MSCs.[4,10–12] Despite several reports being published to establish markers for the ASC phenotype, there is still a lack of consensus over profiles identifying adipose-derived mesenchymal progenitors or osteoprogenitor cells.[13–15] Furthermore, ASCs have been found to exhibit a change in the surface marker phenotype when cultured *in vitro*, which can generate variability in selection of a proper surface marker for osteogenesis.[14,16]

Using single-cell transcriptional analysis, a recent study in our laboratory found expression patterns for the cell surface receptor endoglin (CD105) to be closely associated with osteogenic potential of ASCs.[17] By combining microfluidic analysis with fluorescence-activated cell sorting (FACS), $CD105^{low}$ ASCs were found to be capable of enhanced osteogenic differentiation relative $CD105^{high}$ and unsorted cells. A second cell surface receptor was also found to correlate with expression of osteogenic genes independent from CD105. Known as Thy-1 (CD90), this surface marker is a 25–30 kDa glycosyl-phosphatidylinositol (GPI)-linked membrane protein and has previously been shown to be associated with osteoprogenitor cells.[18–21] The purpose of the present study was to thus compare the ability of CD90 to identify osteoprogenitors relative to CD105. Identifying a cell surface marker associated with enhanced osteogenic capacity would have a profound impact on optimizing cell-based skeletal tissue engineering applications.

Materials and Methods

Cell isolation and culture

Lipoaspiration specimens were obtained after acquiring informed consent from patients, in accordance with the Stanford University Institutional Review Board guidelines. ASCs were harvested from the adipose tissue of two female patients (ages 37 and 48 years) without major medical conditions who were undergoing elective lipoaspiration of the abdomen, flank, and/or thigh region. ASCs were isolated as described previously by Zuk *et al.*[12] Briefly, raw lipoaspirates were washed and treated with 0.075% collagenase type I (Sigma-Aldrich, St. Louis, MO) in the Hank's balanced salt solution (Cellgro, Manassas, VA) for 1 h at 37°C with gentle agitation. The cellular pellet was resuspended and plated onto conventional tissue culture plates in the Dulbecco's modified Eagle's medium (DMEM, High Glucose, GlutaMAX™, HEPES; Life Technologies, Grand Island, NY) supplemented with 10% FBS and 1% P/S.

Fluorescence-activated cell sorting

ASCs were cultured for 36 h before being sorted. The sort was performed on a FACS Aria II instrument (BD Biosciences, San Jose, CA) with the use of a 100-μm nozzle. Briefly, cells were lifted using TrypLE (Invitrogen, Carlsbad, CA) and centrifuged for 5 min at 1000 rpm. The supernatant was discarded by aspiration, and the cells were incubated for 30 min in a flow cytometry buffer (PBS, 2% FBS) containing allophycocyanin-conjugated mouse anti-human CD90 and fluorescein isothiocyanate-conjugated mouse anti-human CD105 antibodies (BD Biosciences). Unsorted cells, $CD90^{+}$, $CD90^{-}$, $CD105^{high}$, and $CD105^{low}$ cells were then seeded at 100,000 cells/well in a six-well plate and treated with the osteogenic differentiation medium (ODM).

In vitro *osteogenic differentiation assay*

For osteogenic differentiation, all assays were performed in triplicate wells. After attachment, cells were grown to at least 80% confluence before being cultured in the ODM, which consisted of the DMEM, High Glucose, GlutaMAX, HEPES supplemented with 10% FBS, 1% P/S, 100 μg/mL ascorbic acid, and 10 mM β-glycerophosphate. Alkaline phosphatase (ALP) staining and quantification were performed at 7 days. Photometric quantification of Alizarin red stain was performed at 14 days to assay extracellular mineralization, as previously described.[22,23]

Reverse transcription and quantitative real-time polymerase chain reaction

RNA from cultivated cells was extracted using the RNeasy Mini Kit (Qiagen, Valencia, CA) according to the manufacturer's protocol. Reverse transcription was performed and osteogenic gene expression was examined by quantitative real-time polymerase chain reaction (qRT-PCR) using the Applied Biosystems Prism 7900HT sequence detection system (Applied Biosystems, Foster City, CA) and SYBR Green PCR Master Mix (Applied Biosystems). The amount of PCR product was calculated using an external GAPDH standard curve and LightCycler software. All values were normalized based on the GAPDH expression in the corresponding samples. Specific primers for the genes examined were based on their PrimerBank sequence.[24]

In vivo *bone formation*

For evaluation of *in vivo* osteogenesis, nonhealing, critical-sized (4-mm) calvarial defects were created in the right

parietal bone of 60-day-old male Crl:CD-1-*Foxn1*^{nu} mice (Charles River Laboratories, Wilmington, MA), as previously described.[25] All research involving vertebrate animals was performed in accordance with approved protocols by Stanford APLAC. Hydroxyapatite (HA)-coated poly(lactic-co-glycolic acid) (PLGA) scaffolds were fabricated from 85/15 poly(lactic-co-glycolic acid) by solvent casting and a particulate leaching process as previously described.[26] In preparation for cell engraftment, scaffolds were seeded with ASCs 24 h before implantation. Each scaffold was implanted alone or was seeded with 150,000 cells in 125 μL of medium in 96-well culture plates and incubated overnight. Animals were treated with the HA-PLGA scaffold seeded with the following cell types: CD90$^+$ ASCs ($n=3$), CD90$^-$ ASCs ($n=3$), CD105^{high} ASCs ($n=3$), and CD105^{low} ASCs ($n=3$). As controls, no scaffold ($n=3$), as well as HA-PLGA scaffolds alone ($n=3$), were used. Before implantation, scaffolds were copiously rinsed with PBS.

For microcomputed tomography (micro-CT) scans, the mice were anesthetized with isoflurane. Imaging was performed using a Siemens Inveon MicroPET/CT scanner (Siemens Medical Solutions, Inc., Malvern, PA). Using our scan protocol parameters, each high-resolution 100-μm image was acquired in a total scan time of 10 min. Mice were scanned immediately, postoperatively and at 2, 4, 6, and 8 weeks following surgery. Data were reconstructed into three-dimensional surfaces using the Siemens Inveon Research Workplace 4.0 Software (Siemens Medical Solutions, Inc., Malvern, PA). The three-dimensional reconstructed images were then analyzed using ImageJ software (Image Processing and Analysis in Java, NIH, Bethesda, MD). The area of the calvarial defects was evaluated by quantifying pixels in the defect. Percentage healing was then determined by dividing the defect area by the defect size immediately postoperatively.

Histological analysis

At 8 weeks postoperatively, calvaria were harvested, immediately fixed in 10% formalin overnight, decalcified in 19% EDTA, dehydrated through an ethanol series, and embedded in paraffin as previously described.[27] Deparaffinized sections were stained with Movat's Pentachrome to detect bone matrix formation. Bright field images were obtained with a 20× objective at room temperature using a Leica DM5000 microscope (Leica Microsystems, Inc., Wetzlar, Germany) equipped with a DFC300FX camera. The images were analyzed using Leica IM1000 Version 4.0 Image Acquisition Software (Leica Microsystems).

Statistical analysis

Numerical data are presented as means ± standard deviations. In figures, bar graphs represent means, and error bars represent one standard deviation. Unless otherwise stated, statistical analysis was performed using a one-way analysis of variance for multiple group comparisons and a two-tailed Student's *t*-test was used to directly compare two groups. The Newman–Keuls and Tukey *post hoc* test were performed using SPSS (Version 16, IBM) to compare the osteogenic potential of all subpopulations. A value of $*p<0.05$ was considered significant.

Results

Fluorescence-activated cell sorting

A strategy using FACS on as few cell surface markers as possible would allow for the largest capture of cells in the shortest amount of time. Because it has been suggested that CD90 and CD105 may be useful as early markers indicating commitment to osteogenic differentiation, we sorted ASCs into CD90$^+$, CD90$^-$, CD105^{high}, CD105^{low}, and unenriched (sorted for live cells only) groups using FACS (Fig. 1A, B). FACS analysis of gated subpopulations at 36 h yielded a CD90$^+$ population comprising 45.7% of the cells and a CD90$^-$ population comprising 46.8% of the cells (Fig. 1B, Left). At this same time point, the CD105^{high} population comprised 43.9% of the cells and the CD105^{low} population comprised 44.7% of the cells (Fig. 1B, Right). Postsort purity analysis revealed over 99.8% enrichment for each population.

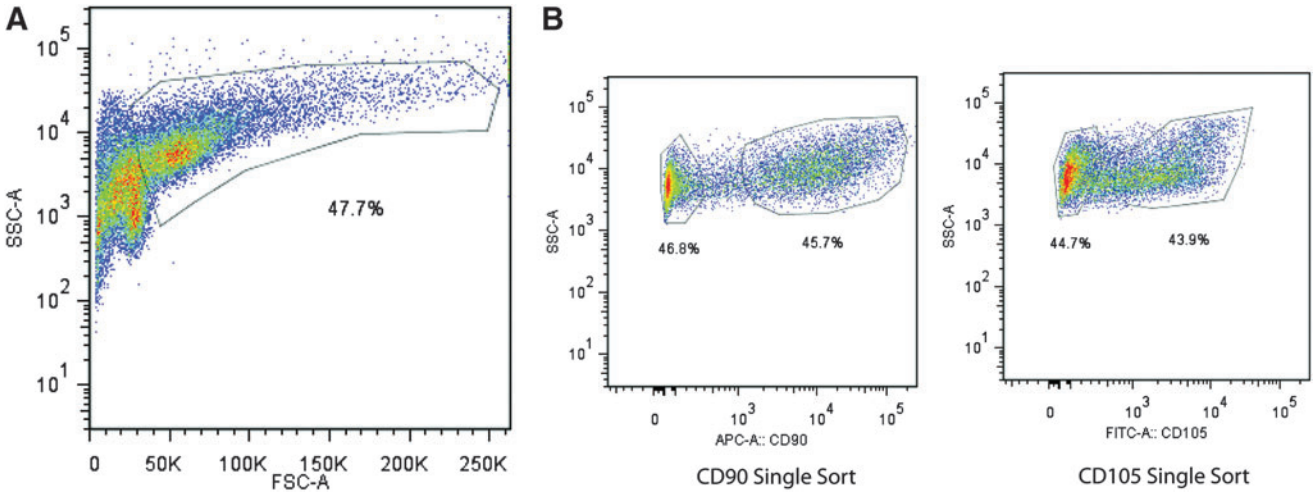

FIG. 1. **(A)** Preliminary cell selection was performed through size and complexity gating to exclude cell debris and to interrogate a focused population. **(B)** Fluorescence-activated cell sorting analysis of CD90 single-sorted (left) and CD105 single-sorted adipose-derived stromal cells (ASCs) (right) 36 h after ASC harvest. Color images available online at www.liebertpub.com/tea

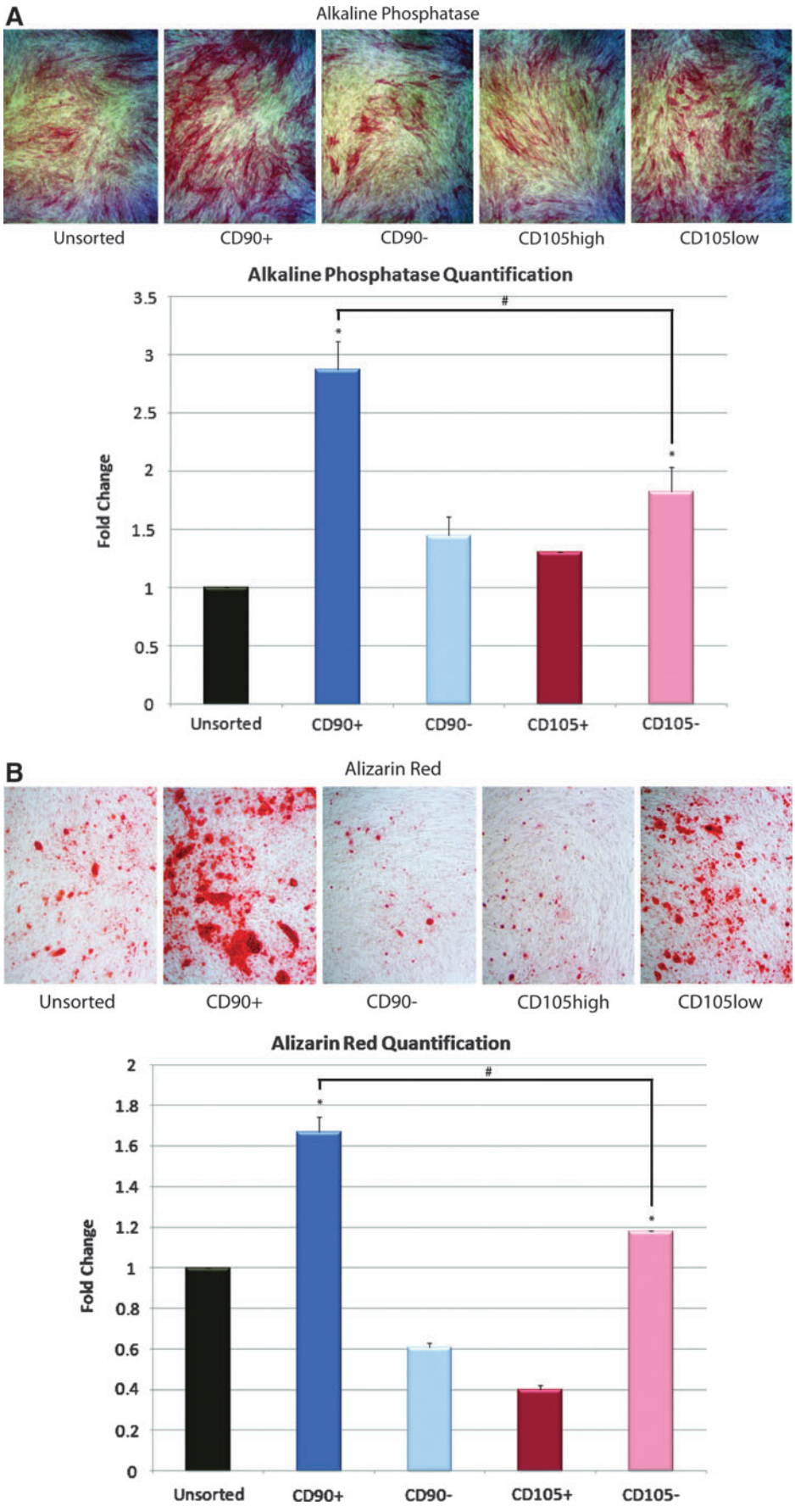

FIG. 2. **(A)** Alkaline phosphatase staining (top) and quantification (bottom) of ASCs at 7 days differentiation. **(B)** Alizarin red stain (top) and quantification (bottom) of ASCs at 14 days differentiation demonstrating increased extracellular matrix mineralization for $CD90^+$ ASCs compared to $CD90^-$ ($^*p < 0.05$) and $CD105^{low}$ cells ($^{\#}p < 0.05$). Color images available online at www.liebertpub.com/tea

In vitro *osteogenic differentiation assay*

To characterize osteogenic potential of the four sorted ASC subpopulations ($CD90^+$, $CD90^-$, $CD105^{high}$, and $CD105^{low}$) as well as the unsorted population *in vitro*, cells were cultured in the ODM for 14 days. Staining at day 7 for ALP, an early marker of bone formation, was significantly increased in the $CD90^+$ population relative to other groups ($^*p<0.05$ and $^{\#}p<0.05$, Figure 2A, Second box). We assessed terminal osteogenic differentiation using Alizarin red staining for extracellular matrix mineralization at day 14 and found that $CD90^+$ ASCs stained significantly greater than $CD90^-$, $CD105^{low}$, or unsorted cells ($^*p<0.05$ and $\#p<0.05$, Fig. 2B).

Osteogenic gene expression

To determine whether this increase in osteogenic differentiation *in vitro* correlated with an increase in osteogenic gene expression, we examined transcript levels for markers of bone differentiation at baseline and after 7 and 14 days of ODM treatment. The $CD90^+$ population demonstrated the greatest upregulation of osteogenic genes Runt-related transcription factor-2 (*RUNX2*), osteopontin (*OPN*), and osteocalcin (*OCN*) ($^*p<0.05$ and $\#p<0.05$, Fig. 3A–C).

In vivo *bone formation*

To evaluate the *in vivo* osteogenic capacity of these ASC populations, repair was performed using $CD90^+$, $CD90^-$, $CD105^{high}$, or $CD105^{low}$ cells seeded onto HA-PLGA scaffolds. Controls included defects treated with an empty scaffold and untreated defects without scaffold or cells. Calvarial defects were analyzed by live microcomputed tomography (micro-CT) from 0 to 8 weeks postoperative as previously described, under isoflurane sedation.[28] Defects treated with $CD90^+$ ASCs demonstrated increased *de novo* bone regeneration when compared with defects treated with $CD90^-$ ASCs, $CD105^{low}$ ASCs, or empty scaffold (Fig. 4A, data not shown). This was observed by high-resolution micro-CT scanning and 3D reconstructions. Serial live micro-CT scans were performed every 2 weeks postoperatively and percentage of healing based on the size of the original defect was quantified using ImageJ software. Quantification of healing at 2, 4, 6, and 8 weeks postoperatively demonstrated significantly increased bone formation in defects treated with $CD90^+$ ASCs when compared with all other groups ($^*p<0.05$ and $\#p<0.05$, Fig. 4B).

Histological analysis

Histological analysis with Movat's Pentachrome staining (in which mature bone stains yellow) of calvarial defects at 8 weeks postsurgery correlated with micro-CT findings. Defects treated with $CD90^+$ cells showed robust and thick bony regeneration throughout the defect. Defects treated with $CD90^-$ cells, $CD105^{high}$ cells, and $CD105^{low}$ cells demonstrated some bone formation, but to a lesser degree when compared with the $CD90^+$ group (Fig. 5).

Discussion

At present, prospective enrichment of the SVF of human adipose tissue to isolate homogenous stem cell subpopulations remains elusive. For the purpose of bone regeneration, selection of a proper surface marker for osteogenesis is imperative. Using single-cell transcriptional analysis to determine correlations between expression of various surface markers and clusters of osteogenic transcriptional activity, we had found both endoglin (CD105) and Thy-1 (CD90) to be associated with differences in expression of osteogenic genes among ASCs.[17] In the present study, we used ASCs at a similar time point of 36 h after harvest and isolated four ASC subpopulations ($CD90^+$, $CD90^-$, $CD105^{high}$, and $CD105^{low}$) by FACS.

Thy-1 (CD90) is a member of the immunoglobulin (Ig) supergene family with structural similarity to the Ig V_H

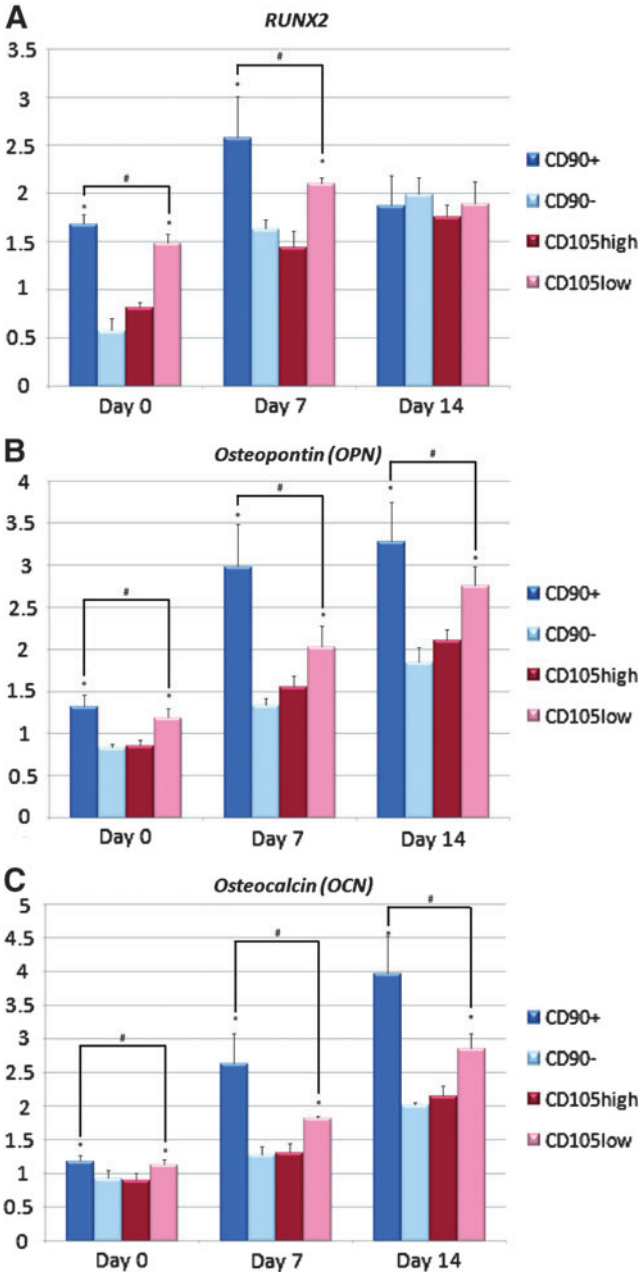

FIG. 3. Gene expression of **(A)** early (*RUNX2*), **(B)** intermediate (*OPN*), and **(C)** late (*OCN*) osteogenic markers. Across all genes at each time point, $CD90^+$ cells had greater expression relative to $CD90^-$ ($^*p<0.05$) and $CD105^{low}$ cells ($^{\#}p<0.05$). Color images available online at www.liebertpub.com/tea

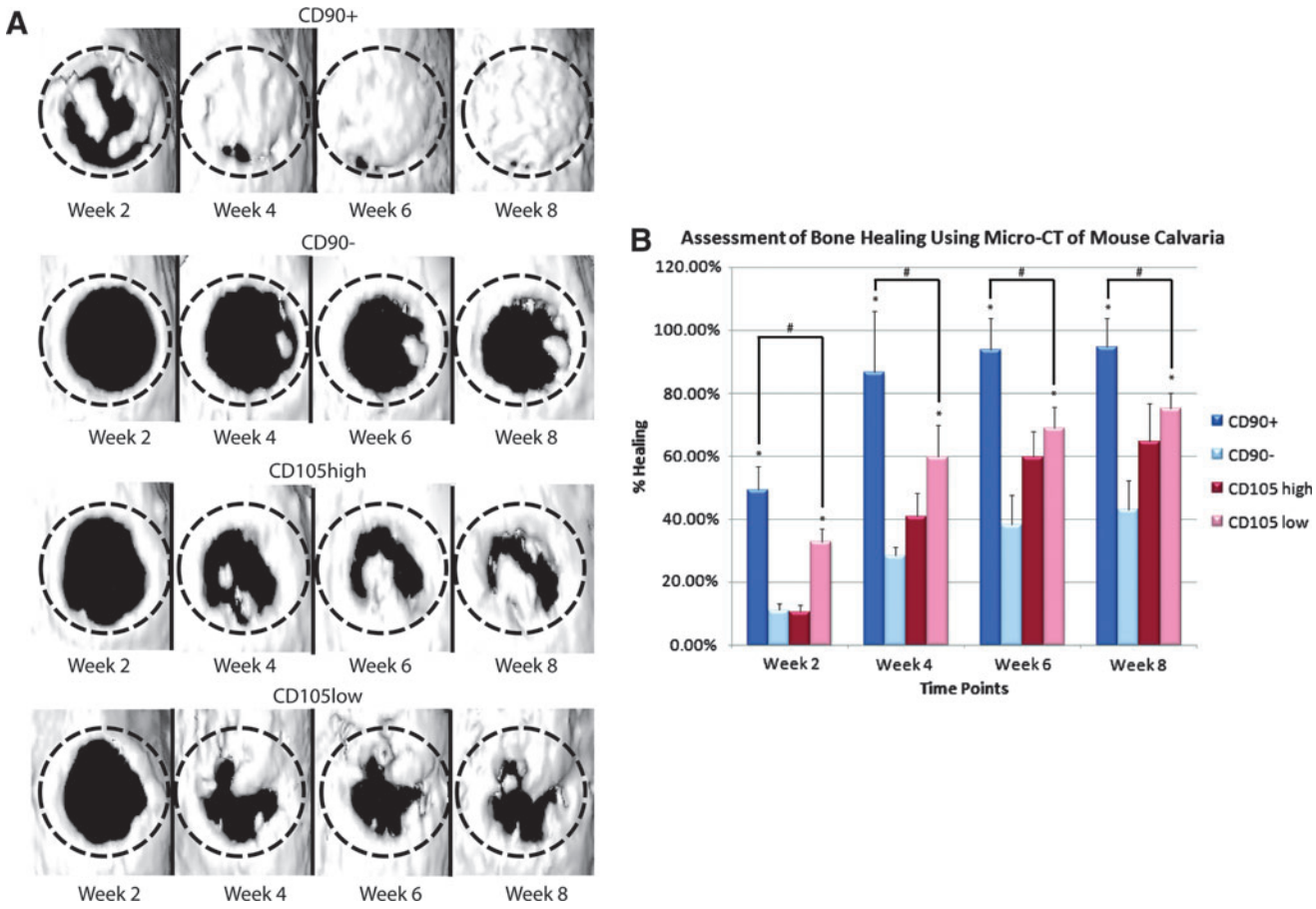

FIG. 4. **(A)** Three-dimensional reconstruction of calvarial defects. Mice were scanned at 2, 4, 6, and 8 weeks following surgery. At each time point, the $CD90^+$-treated defects demonstrated improved bone healing. **(B)** Quantification of osseous healing by micro-CT revealed significantly more healing with $CD90^+$ cells relative to $CD90^-$ ($*p < 0.05$) and $CD105^{low}$ cells ($\#p < 0.05$) cells at the 2-, 4-, 6-, and 8-week time points. Color images available online at www.liebertpub.com/tea

region domain.[29,30] The molecule is a 25–30 kDa GPI-linked membrane glycoprotein encoded by a single gene on chromosome 11 in humans.[31,32] CD90 is expressed in a tissue-specific and developmentally controlled manner. This glycoprotein is expressed on the surfaces of thymocytes, peripheral T cells, fibroblasts, epithelial cells, neurons, and hematopoietic stem cells.[33–35] Chen *et al.* reported that CD90 expression appeared to change with the state of differentiation of cells in the osteoblast lineage. The highest levels of constitutive expression was observed on proliferating cells and decreased once the cells progressed through the matrix maturation and mineralization stages.[19]

CD90 and CD105 have been identified as early MSC markers present on both BM-MSCs and ASCs. Similar to previous findings, in freshly isolated SVF of adipose tissue, the $CD90^+$ population represented ~50% of cells.[36] Immediately after ASC harvest, however, only ~5%–10% of the initial SVF cell population expressed CD105.[17,36] Importantly, with successive passages, the percentage of cells staining positive for CD105 increased.[17,36] It is known that ASCs exhibit a shift in phenotypic expression under *in vitro* conditions, which may alter the biology of stem cells.[17,37–41] Thus, for clinical applications, it would be optimal to obtain a highly purified cell population for direct transplantation or cell seeding to a scaffold without the need for *in vitro* cultivation.

Levi *et al.* highlighted the functional significance of CD105 with respect to the molecular mechanism behind osteogenic differentiation.[17] They concluded that CD105 depletion was found to enhance osteogenesis through reduction of transforming growth factor-β1 signaling, a known inhibitor of mesenchymal cell osteogenic differentiation. However, even after 7 days of *in vitro* culture, the $CD105^{low}$ cells, which would have undergone phenotypic drift (toward increased expression of CD105), did not lose their osteogenic capacity. Furthermore, conflicting data exists on the correlation of CD105 expression and osteogenic differentiation capacity.[41–43] Aslan *et al.* found that $CD105^+$ cells exhibited enhanced *in vitro* osteogenic differentiation.[42] Similarly, Jarocha *et al.* observed that expanded $CD105^+$ populations showed higher levels of early (*RUNX2*) and late (*OCN*) molecular markers for osteogenic progenitors.[44] Dennis *et al.* took things one step further and found that there was a good correlation between *in vitro* mineralization and *in vivo* osteogenesis for $CD105^+$ cells.[45] Interestingly, Dennis *et al.* also found a clear correlation of $CD105^+$ cell numbers with *in vivo* bone scores, suggesting that the overall frequency of specific cell types seems to be an important parameter in predicting the osteogenic potential of

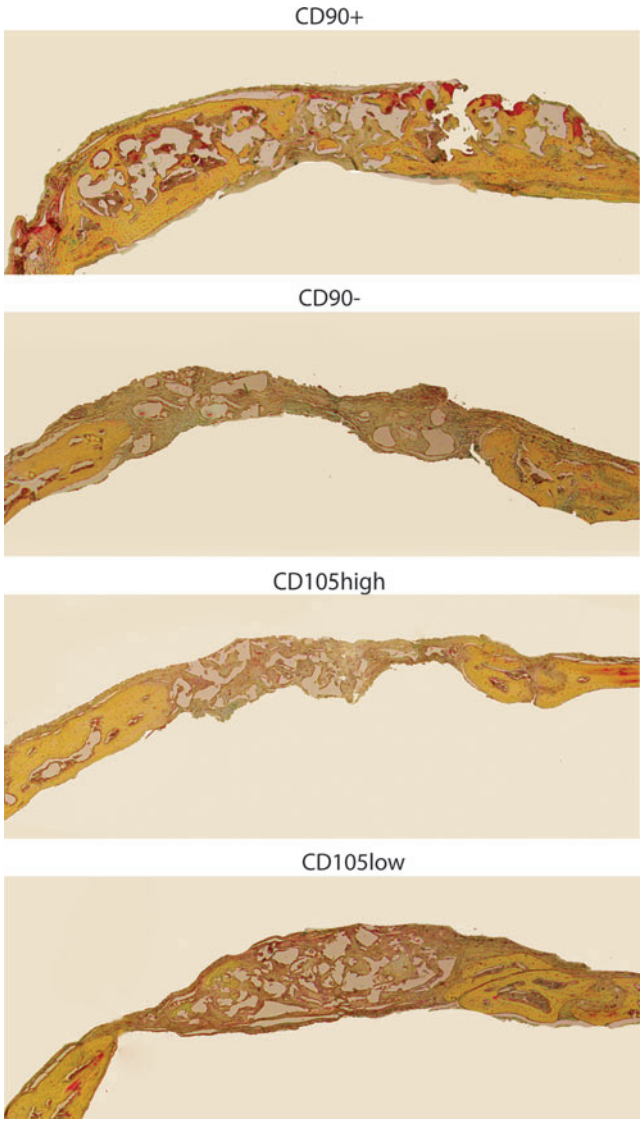

FIG. 5. Calvarial defects 4 mm in size were allowed to heal for 8 weeks before histological analysis by Movat's Pentachrome staining. Pictures were taken in the middle of the defect site. In pentachrome stains, bone appears yellow. Color images available online at www.liebertpub.com/tea

cells. Although these studies examined a different cell type (BM-MSCs), Jiang *et al.* observed the same findings in ASCs.[46] After 14 days of osteogenic induction, a much stronger osteogenic-specific staining was observed in the $CD105^+$ group compared to the $CD105^-$ group.[46]

On the contrary, several studies have demonstrated that adult stem cells expressing CD90 possess high potential to undergo osteogenic differentiation. To investigate the relationship between CD90 expression and osteoblastic differentiation more precisely, Nakamura *et al.* cultured cells under osteogenic conditions and analyzed the expression levels of CD90 and osteoblastic markers.[21] While $CD90^+$ cells were capable of robust osteogenic differentiation, qRT-PCR demonstrated that CD90 expression decreased as calcified nodules formed. Similarly, Hosoya *et al.* evaluated the capacity of $CD90^+$ and $CD90^-$ subodontoblastic dental pulp stem cells to differentiate into hard tissue-forming cells *in vitro* and *in vivo*.[20] In concert with our findings in the present study, they found that $CD90^+$ cells showed accelerated induction of ALP activity and formation of alizarin red-positive mineralized matrix compared to $CD90^-$ cells. Furthermore, subcutaneous implantation of $CD90^+$ cells efficiently induced the formation of bone-like matrix *in vivo*.

Importantly, the correlation of CD90 with bone formation supports the findings of Chen *et al.*, who proposed that CD90 expression on osteoblast-like cells may be used to help follow the development of the osteoblast lineage.[19] This finding has further been supported by subsequent studies showing that CD90 is only transiently expressed during the differentiation of MSCs to osteoblast-like cells.[47,48] Application of mechanical stimulation is known to change the phenotypic expression of cells.[49] Wiesmann *et al.* found that when human MSCs were cultured in the osteoinductive medium with cyclic uniaxial mechanical stimulation, CD90 expression decreased, while there was an increase of collagen I, osteonectin, and osteocalcin.[48] Using a microcell stimulator designed to culture and apply mechanical stimulation to human MSCs, and Sim *et al.* also showed that CD90 expression was maximal at the earliest stage of maturation, during the proliferative phase, and then declined as the cells matured.[47] Similar analysis of CD105 failed to demonstrate any distinct differences between the control group and the stimulation group.

In the present study, we enriched for four ASC subpopulations ($CD90^+$, $CD90^-$, $CD105^{high}$, and $CD105^{low}$) to evaluate their relative capacity to undergo osteogenic differentiation *in vitro* and *in vivo* when implanted onto HA-PLGA scaffolds. We demonstrated that $CD90^+$ cells have enhanced osteogenic potential *in vitro* and *in vivo* when compared with $CD90^-$, $CD105^{low}$, $CD105^{high}$, or unsorted cells. Our findings from the *in vitro* osteogenic differentiation assays correlated well with qRT-PCR data, which showed that the $CD90^+$ population demonstrated upregulation of the osteogenic genes *RUNX2*, *OCN*, and *OPN*. To our knowledge, this is the first study to perform a direct comparative analysis of two cell surface markers and their ability to predict a high capacity for osteogenic differentiation *in vitro* and *in vivo* using human ASCs. Our findings demonstrate that CD90 may be a better marker than CD105 to isolate osteogenic cells. It is our hope that this approach may provide a sound base for cell-based strategies for bone tissue engineering.

Author Contributions

M.T.C. and D.C.W. contributed to the project design, data acquisition, drafted and revised the article, and approved the final version. M.T.C., C.L., J.S.H, D.D.L., D.T.M, M.H., M.S., and R.R. contributed to acquisition of data, revision of the article, and final approval. S.L., M.K., F.Y., and N.Q. contributed to analysis of data, revision of the article, and final approval. D.C.W. and M.T.L. contributed to the project design and conception, interpretation of data, revision of the article, and approval of the final version.

Acknowledgments

This study was supported by National Institutes of Health Research grant R01-DE021683-01 to M.T.L and R01-DE019434 to M.T.L; Howard Hughes Medical Institute Research Fellowship to M.T.C.

Disclosure Statement

None of the authors have a financial interest in any of the products, devices, or drugs mentioned in this manuscript. None of the authors have any competing financial interest to report.

References

1. Friedenstein, A.J., Chailakhyan, R.K., Latsinik, N.V., Panasyuk, A.F., and Keiliss-Borok, I.V. Stromal cells responsible for transferring the microenvironment of the hemopoietic tissues. Cloning *in vitro* and retransplantation *in vivo*. Transplantation **17,** 331, 1974.
2. Friedenstein, A.J., Deriglasova, U.F., Kulagina, N.N., Panasuk, A.F., Rudakowa, S.F., Luria, E.A., *et al.* Precursors for fibroblasts in different populations of hematopoietic cells as detected by the *in vitro* colony assay method. Exp Hematol **2,** 83, 1974.
3. Zuk, P.A., Zhu, M., Mizuno, H., Huang, J., Futrell, J.W., Katz, A.J., *et al.* Multilineage cells from human adipose tissue: implications for cell-based therapies. Tissue Eng **7,** 211, 2001.
4. Gronthos, S., Franklin, D.M., Leddy, H.A., Robey, P.G., Storms, R.W., and Gimble, J.M. Surface protein characterization of human adipose tissue-derived stromal cells. J Cell Physiol **189,** 54, 2001.
5. Halvorsen, Y.C., Wilkison, W.O., and Gimble, J.M. Adipose-derived stromal cells—their utility and potential in bone formation. Int J Obes Relat Metab Disord 24 Suppl **4,** S41, 2000.
6. Halvorsen, Y.D., Franklin, D., Bond, A.L., Hitt, D.C., Auchter, C., Boskey, A.L., *et al.* Extracellular matrix mineralization and osteoblast gene expression by human adipose tissue-derived stromal cells. Tissue Eng **7,** 729, 2001.
7. Aust, L., Devlin, B., Foster, S.J., Halvorsen, Y.D., Hicok, K., du Laney, T., *et al.* Yield of human adipose-derived adult stem cells from liposuction aspirates. Cytotherapy **6,** 7, 2004.
8. Yamamoto, T., Gotoh, M., Hattori, R., Toriyama, K., Kamei, Y., Iwaguro, H., *et al.* Periurethral injection of autologous adipose-derived stem cells for the treatment of stress urinary incontinence in patients undergoing radical prostatectomy: report of two initial cases. Int J Urol **17,** 75, 2010.
9. Locke, M., Feisst, V., and Dunbar, P.R. Concise review: human adipose-derived stem cells: separating promise from clinical need. Stem Cells **29,** 404, 2011.
10. Deans, R.J., and Moseley, A.B. Mesenchymal stem cells: biology and potential clinical uses. Exp Hematol **28,** 875, 2000.
11. Pittenger, M.F., Mackay, A.M., Beck, S.C., Jaiswal, R.K., Douglas, R., Mosca, J.D., *et al.* Multilineage potential of adult human mesenchymal stem cells. Science **284,** 143, 1999.
12. Zuk, P.A., Zhu, M., Ashjian, P., De Ugarte, D.A., Huang, J.I., Mizuno, H., *et al.* Human adipose tissue is a source of multipotent stem cells. Mol Biol Cell **13,** 4279, 2002.
13. Lin, C.S., Xin, Z.C., Deng, C.H., Ning, H., Lin, G., and Lue, T.F. Defining adipose tissue-derived stem cells in tissue and in culture. Histol Histopathol **25,** 807, 2010.
14. Zannettino, A.C., Paton, S., Arthur, A., Khor, F., Itescu, S., Gimble, J.M., *et al.* Multipotential human adipose-derived stromal stem cells exhibit a perivascular phenotype *in vitro* and *in vivo*. J Cell Physiol **214,** 413, 2008.
15. Zimmerlin, L., Donnenberg, V.S., Pfeifer, M.E., Meyer, E.M., Peault, B., Rubin, J.P., *et al.* Stromal vascular progenitors in adult human adipose tissue. Cytometry A **77,** 22, 2010.
16. Yoshimura, K., Shigeura, T., Matsumoto, D., Sato, T., Takaki, Y., Aiba-Kojima, E., *et al.* Characterization of freshly isolated and cultured cells derived from the fatty and fluid portions of liposuction aspirates. J Cell Physiol **208,** 64, 2006.
17. Levi, B., Wan, D.C., Glotzbach, J.P., Hyun, J., Januszyk, M., Montoro, D., *et al.* CD105 protein depletion enhances human adipose-derived stromal cell osteogenesis through reduction of transforming growth factor beta1 (TGF-beta1) signaling. J Biol Chem **286,** 39497, 2011.
18. Chan, C.K., Chen, C.C., Luppen, C.A., Kim, J.B., DeBoer, A.T., Wei, K., *et al.* Endochondral ossification is required for haematopoietic stem-cell niche formation. Nature **457,** 490, 2009.
19. Chen, X.D., Qian, H.Y., Neff, L., Satomura, K., and Horowitz, M.C. Thy-1 antigen expression by cells in the osteoblast lineage. J Bone Miner Res **14,** 362, 1999.
20. Hosoya, A., Hiraga, T., Ninomiya, T., Yukita, A., Yoshiba, K., Yoshiba, N., *et al.* Thy-1-positive cells in the subodontoblastic layer possess high potential to differentiate into hard tissue-forming cells. Histochem Cell Biol, 2012.
21. Nakamura, H., Yukita, A., Ninomiya, T., Hosoya, A., Hiraga, T., and Ozawa, H. Localization of Thy-1-positive cells in the perichondrium during endochondral ossification. J Histochem Cytochem **58,** 455, 2010.
22. Wang, Y., Zhao, L., and Hantash, B.M. Support of human adipose-derived mesenchymal stem cell multipotency by a poloxamer-octapeptide hybrid hydrogel. Biomaterials **31,** 5122, 2010.
23. Wang, Y.H., Ho, M.L., Chang, J.K., Chu, H.C., Lai, S.C., and Wang, G.J. Microporation is a valuable transfection method for gene expression in human adipose tissue-derived stem cells. Mol Ther **17,** 302, 2009.
24. Wang, X., and Seed, B. A PCR primer bank for quantitative gene expression analysis. Nucleic Acids Res **31,** e154, 2003.
25. Gupta, D.M., Kwan, M.D., Slater, B.J., Wan, D.C., and Longaker, M.T. Applications of an athymic nude mouse model of nonhealing critical-sized calvarial defects. J Craniofac Surg **19,** 192, 2008.
26. Cowan, C.M., Shi, Y.Y., Aalami, O.O., Chou, Y.F., Mari, C., Thomas, R., *et al.* Adipose-derived adult stromal cells heal critical-size mouse calvarial defects. Nat Biotechnol **22,** 560, 2004.
27. Levi, B., James, A.W., Nelson, E.R., Vistnes, D., Wu, B., Lee, M., *et al.* Human adipose derived stromal cells heal critical size mouse calvarial defects. PLoS One **5,** e11177, 2010.
28. Hsu, W.K., Virk, M.S., Feeley, B.T., Stout, D.B., Chatziioannou, A.F., and Lieberman, J.R. Characterization of osteolytic, osteoblastic, and mixed lesions in a prostate cancer mouse model using 18F-FDG and 18F-fluoride PET/CT. J Nucl Med **49,** 414, 2008.
29. McKenzie, J.L., and Fabre, J.W. Human thy-1, unusual localization and possible functional significance in lymphoid tissues. J Immunol **126,** 843, 1981.
30. McKenzie, J.L., and Fabre, J.W. Distribution of Thy-1 in human brain: immunofluorescence and absorption analyses with a monoclonal antibody. Brain Res **230,** 307, 1981.
31. Ingraham, H.A., and Evans, G.A. Characterization of two atypical promoters and alternate mRNA processing in the mouse Thy-1.2 glycoprotein gene. Mol Cell Biol **6,** 2923, 1986.
32. Ingraham, H.A., Lawless, G.M., and Evans, G.A. The mouse Thy-1.2 glycoprotein gene: complete sequence and identification of an unusual promoter. J Immunol **136,** 1482, 1986.
33. Blankenhorn, E.P., and Douglas, T.C. Location of the gene for Theta antigen in the mouse. J Hered **63,** 259, 1972.
34. Reif, A.E., and Allen, J.M. Immunological Distinction of Akr Thymocytes. Nature **203,** 886, 1964.

35. Williams, A.F. Surface molecules and cell interactions. J Theor Biol **98,** 221, 1982.
36. Mitchell, J.B., McIntosh, K., Zvonic, S., Garrett, S., Floyd, Z.E., Kloster, A., *et al.* Immunophenotype of human adipose-derived cells: temporal changes in stromal-associated and stem cell-associated markers. Stem Cells **24,** 376, 2006.
37. McMurray, R.J., Gadegaard, N., Tsimbouri, P.M., Burgess, K.V., McNamara, L.E., Tare, R., *et al.* Nanoscale surfaces for the long-term maintenance of mesenchymal stem cell phenotype and multipotency. Nat Mater **10,** 637, 2011.
38. Katz, A.J., Tholpady, A., Tholpady, S.S., Shang, H., and Ogle, R.C. Cell surface and transcriptional characterization of human adipose-derived adherent stromal (hADAS) cells. Stem Cells **23,** 412, 2005.
39. McIntosh, K., Zvonic, S., Garrett, S., Mitchell, J.B., Floyd, Z.E., Hammill, L., *et al.* The immunogenicity of human adipose-derived cells: temporal changes *in vitro*. Stem Cells **24,** 1246, 2006.
40. Rada, T., Gomes, M.E., and Reis, R.L. A novel method for the isolation of subpopulations of rat adipose stem cells with different proliferation and osteogenic differentiation potentials. J Tissue Eng Regen Med **5,** 655, 2011.
41. Rada, T., Reis, R.L., and Gomes, M.E. Distinct stem cells subpopulations isolated from human adipose tissue exhibit different chondrogenic and osteogenic differentiation potential. Stem Cell Rev **7,** 64, 2011.
42. Aslan, H., Zilberman, Y., Kandel, L., Liebergall, M., Oskouian, R.J., Gazit, D., *et al.* Osteogenic differentiation of noncultured immunoisolated bone marrow-derived CD105+ cells. Stem Cells **24,** 1728, 2006.
43. Bernabeu, C., Conley, B.A., and Vary, C.P. Novel biochemical pathways of endoglin in vascular cell physiology. J Cell Biochem **102,** 1375, 2007.
44. Jarocha, D., Lukasiewicz, E., and Majka, M. Adventage of mesenchymal stem cells (MSC) expansion directly from purified bone marrow CD105+ and CD271+ cells. Folia Histochem Cytobiol **46,** 307, 2008.
45. Dennis, J.E., Esterly, K., Awadallah, A., Parrish, C.R., Poynter, G.M., and Goltry, K.L. Clinical-scale expansion of a mixed population of bone-marrow-derived stem and progenitor cells for potential use in bone-tissue regeneration. Stem Cells **25,** 2575, 2007.
46. Jiang, T., Liu, W., Lv, X., Sun, H., Zhang, L., Liu, Y., *et al.* Potent *in vitro* chondrogenesis of CD105 enriched human adipose-derived stem cells. Biomaterials **31,** 3564, 2010.
47. Sim, W.Y., Park, S.W., Park, S.H., Min, B.H., Park, S.R., and Yang, S.S. A pneumatic micro cell chip for the differentiation of human mesenchymal stem cells under mechanical stimulation. Lab Chip **7,** 1775, 2007.
48. Wiesmann, A., Buhring, H.J., Mentrup, C., and Wiesmann, H.P. Decreased CD90 expression in human mesenchymal stem cells by applying mechanical stimulation. Head Face Med **2,** 8, 2006.
49. Perka, C., Schultz, O., Spitzer, R.S., and Lindenhayn, K. The influence of transforming growth factor beta1 on mesenchymal cell repair of full-thickness cartilage defects. J Biomed Mater Res **52,** 543, 2000.

Address correspondence to:
Derrick C. Wan, MD
Hagey Laboratory for Pediatric Regenerative Medicine
Plastic and Reconstructive Surgery Division
Department of Surgery
Stanford University School of Medicine
257 Campus Drive
Stanford University
Stanford, CA 94305-5148

E-mail: dwan@stanford.edu

Received: June 13, 2012
Accepted: November 8, 2012
Online Publication Date: January 28, 2013